COMPUTERS IN CARDIOLOGY

September 23-25, 1981
Florence, Italy

L81-29

IEEE Catalog No. 81CH1750-9
Library of Congress No. 80-691097
Computer Society No. 384
ISSN No. 0276-6574

LUNG DENSITY IMAGING IN PULMONARY EDEMA: CHEST X-RAY VERSUS COMPTON SCATTER TOMOGRAPHY

Miniati M.*, Pistolesi M.*, Solfanelli S.*, Giuntini C.**
Azzarelli L.***, Chimenti M.***, Denoth F.***, Fabbrini F.***

*C.N.R. Institute of Clinical Physiology, Pisa
** 2nd Medical Clinic University of Pisa
*** C.N.R. Institute for Elaboration of Information, Pisa, Italy

In the course of pulmonary edema water accumulates in the extravascular space with a consequent increase of lung density. Therefore, the severity of the disease may be quantified and the time course followed if lung density changes can be measured. A tomographic technique was developed in order to visualize sectional chest planes by means of a collimated linear source of gamma rays and a gamma camera to detect Compton scattered photons at 90° to the primary beam. As the intensity of the Compton effect is a linear function of the scanned tissue density, the resulting image is a map of the distribution of lung densities along the plane crossed by the incident beam. A computer processing of the original images was performed to clear the views of systematic and/or random acquisition errors. The application of this technique to the study of pulmonary edema and the comparison with x-ray findings are described.

Pulmonary edema can be defined as an abnormal accumulation of fluid and solute in the extravascular space of the lung. This process has two main consequences: on the pathophysiological ground there is a progressive distension of the loose connective tissue around vessels and airways since the fluid, produced at the level of the exchanging vessels, is shifted towards this space that behaves like a sequestered pool slowly mixing with the microvascular filtrate[1]. The progressive recruitment of the extravascular space gives rise to specific morphological features such as perivascular and peribronchial cuffs that can be easily recognized on the plain chest film, the most used and simplest method to detect pulmonary edema. Indeed chest x-ray has been shown to be sensitive to reveal subtle signs of interstitial fluid accumulation when the actual amount of extravascular water is only slightly above the normal range[2]. As a second consequence the development of edema fluid induces a change in the physical properties of the lung tissue i.e. in its density. Under physiological conditions, lung density is the result of three different elements: gas, intravascular blood and tissue density. In the course of pulmonary edema the accumulation of fluid in the extravascular space, by replacing the gas density with a water equivalent density, yields a progressive increase of the overall lung density. As chest x-ray does not provide an objective assessment of the distribution of the increased lung density, many attempts have been made so far to obtain a correct measurement of this parameter "in vivo" by using either radiologic or isotopic methods. Computerized axial tomography[3] (CAT) provides images of transverse sections of the thorax by measuring the relative x-ray absorption by chest tissue. The resulting tomograms show an accurate anatomic definition of the intrathoracic structures but require a significant radiation load to the patient. Moreover the Hounsfield scale for tissue density display does not allow an immediate comparison with the actual gravimetric tissue density. Furthermore CAT scanners cannot be used in an intensive care unit to monitor day to day changes of lung density. Isotopic techniques, such as those based on the Compton scatter effect[4], yield a measurement of the absolute density of a small portion of lung volume but cannot provide an image of the regional distribution of the lung density increment.

Likewise, methods based on the transthoracic gamma-rays attenuation[5], though simple and reproducible, do not give any information about the distribution patterns of lung edema. Recently a tomographic technique has been developed to detect lung density changes in various clinical disorders. Sectional planes of the chest are visualized, according to their density, by means of a collimated linear source of gamma rays and a gamma camera as imaging device to detect Compton Scatter at 90° to the primary beam[6].

Compton scatter tomography

The source of gamma rays (^{192}Ir) has a multienergetic emission with an average value of 307 KeV, therefore within a range where, for an inter-

0276-6574/81/0000/0069$00.75 © 1982 IEEE

action with human tissues, the Compton scatter is one order of magnitude greater than the photoelectric effect. The energy of the 90° scattered photons (195 Kev) is suitable for detection with an imaging device such as a gamma camera. Furthermore the emitter's half life (74.4 days) is long enough to allow the use of the source for 3 months when the initial activity is about 1.5 Curies. The ^{192}Ir source is shielded in a lead box with the exception for a 3 mm wide slit through which the primary beam is appropriately collimated. Fig. 1 shows the spatial relationships among the gamma source, the detecting device and the patient in order to obtain frontal and sagittal sections of the chest.

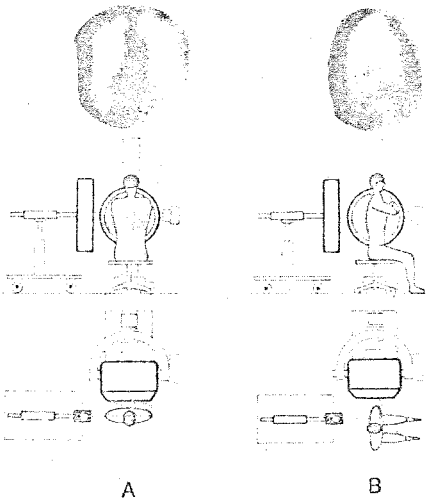

Fig. 1: set up of the Compton scattering technique to obtain frontal (A) and sagittal (B) tomograms of the chest.

Images can be recorded either in the seated or supine posture as the gamma source can be rotated, moved up and down and wheeled around. These facilities enable to obtain a bedside measurement of lung density even in severely ill patients, particularly when a portable gamma camera is available. Tomographic views with 500,000 counts are collected on a 35 mm photographic film in 1-2 minutes, at the spatial resolution of the gamma camera, with a tissue density discrimination of 12% as proved by phantom studies.

The radiation load to the patient is estimated about 0.09 Rads per view i.e. well below the values of conventional and computerized x-Ray tomography. As the intensity of the Compton scattering is a linear function of the electron density of the scanned tissue, the tomographic images will provide a map of the distribution of lung density along the plane travelled by the incident beam. However, original images are affected by several systematic or random errors: divergence and non uniformity of the radiation source, non uniformity of the detecting device, primary beam attenuation, 90°Compton scattered beam attenuation, multiple scattering, room and detector noise, photographic process. In order to clear the views of these errors a computer processing is performed on the acquired data.

Computer processing of the original data

Photographic images are digitized by means of a flying spot and then processed by a computer program (7). Digitized data are a measure of the photogram optical density. The gravimetric density of the scanned tissue is obtained by means of the relation N = f(D) which defines the counting density of gamma camera, N, as a function of the optical density, D, of the photographic film. The relationship is obtained by keeping constant the exposure time To and varying the intensity Ic of the radiation detected by the gamma camera. We then obtain eq. 1:

$$N = Ic.To \qquad (1)$$

where N ≡ number of counts.cm^{-2}

Ic≡ number of counts.sec^{-1}.cm^{-2}

To≡ seconds

The relationship between density D and the radiation intensity Ic is then obtained. The fluence of 90° scattered photons from a single volume element can be expressed by eq. 2:

$$Ic = I_o.k.\rho_e \qquad (2)$$

where Ic = 90° scattered radiation intensity

I_o = incident radiation intensity

k^o = 90° scattering coefficient, depending on the Klein-Nishina cross-section function

ρ_e = electron density of the volume element

The intensity of the scattered radiation is then proportional to the density ρ_e of the single volume element. By means of equation (1) it is possible to recover the density distribution $\rho(x,y)$ of the scanned target from the measured values of optical density. For sake of simplicity the gravimetric tissue density has been assumed to be numerically equal to the electron density ρ_e.

The measured density values depend on Io as shown in equation (2). However when a large block of material is irradiated, the intensity of the incident radiation decreases as a function of the distance travelled along the target.

The resulting density values are therefore considerably distorted. For example, in an uniform material we have:

$$I_o(x) = I_o . e^{-\mu x}$$

where μ = attenuation coefficient
x = thickness of the attenuating material

The apparent density $\rho(x)$ becomes:

$$\rho(x) = \rho_o . e^{-\mu(x)}$$

where $\rho_o = \rho|_{x=o}$

A typical density distribution along a sagittal tomogram of the human chest is shown in fig. 2.

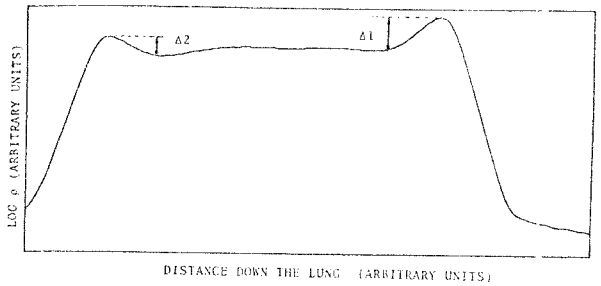

Fig. 2: Profile of a sagittal cross-section of the human chest (uncorrected)

The two high density peaks correspond to the chest walls, whereas the low-level zone corresponds to the lung tissue. The value of $\rho(x)$ decreases according to the primary beam attenuation as stated above. $\rho(x)$ is plotted on a logarithmic scale, so that a linear attenuation is obtained. Moreover, we can see that Δ_1 that is the difference between the density of the chest wall and that of the lung tissue close to the gamma source, is greather than Δ_2 at the opposite site. This can be due multiple scattering of the radiation within the chest tissue. It has been shown[8] that multiple scattering increases as a function of the depth of the incident radiation in the scanned tissue.

This yields a reduction of the spatial and photometric resolution of the acquired image. In order to obtain correct data of gravimetric density, a digital procedure has been implemented based on two assumptions:

1) actual chest wall density should be the same and equal to one.
2) Δ_1 and Δ_2 should be equal.

Fig. 3 shows the same profile of fig. 2 after the computer processing. Density values are expressed on a linear scale and are normalized with respect to the chest wall tissue density.

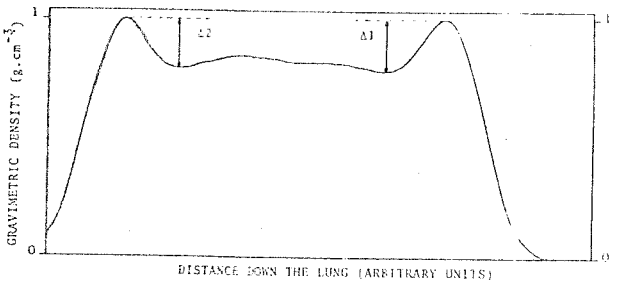

Fig. 3.: Profile of the same section (corrected).

Clinical applications

In 12 patients with cardiogenic pulmonary edema we compared chest x-ray findings with Compton scatter tomography. Both techniques show a predominantly central perihilar distribution of the increased lung density. However, while chest x-ray is apt to reveal subtle signs of interstitial fluid accumulation, Compton scatter tomography is more reliable to detect regional and time-related density changes, expression of the edema fluid dynamics in the extravascular space. Some examples are reproduced to stress the distinctive features of these technique.

In fig. 4 the plain chest film of a patient with mitral stenosis reveals specific signs of interstitial edema such as peribronchial and perivascular cuffs, septal lines and micronoduli. Hilar vessels are blurred and markedly increased in size and density. Upper lobe veins are dilated, thus indicating a clear cut redistribution of blood flow towards the apices.

Fig. 4.: Chest x-ray of a patient with mitral stenosis and interstitial pulmonary edema.

Sagittal tomographic images of the left lung (fig. 5) clearly outline the regional distribution of the increased lung density, that is predominantly located in the paramediastinal sections (upper row) around the large hilar vessels and in the dependent zones of the lung, with a relative sparing of the cortical, more peripheral regions. An intrafissural collection of fluid is followed in its tridimensional shape throughout the whole depth of the lung. This finding, along with the change in shape of the chest walls at different depths and the progressive disappearance of the heart shadow in the peripheral tomograms, emphasize the effective tomographic properties of the technique.

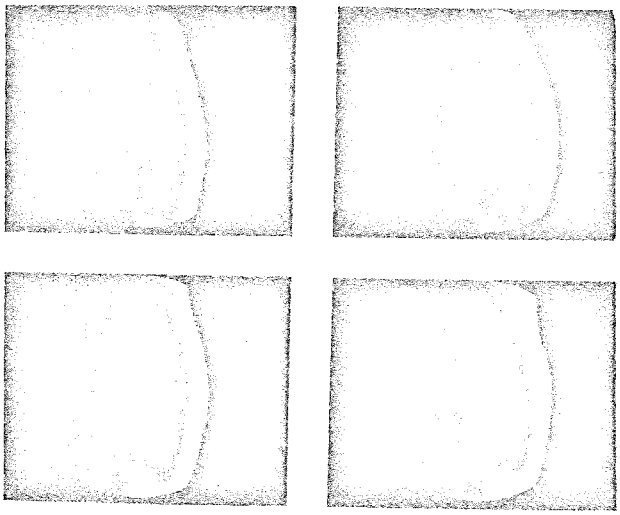

Fig. 5.: Left lung sagittal tomograms of the same patient.

Fig. 6 shows the chest x-ray of a patient with congestive cardiomyopathy and severe lung edema. In the posteroanterior view an extensive perihilar haze, predominantly on the right side, is observed which obscures the hilar vessels and the right cardiac border. On the lateral view signs of intrafissural fluid collection and a right sided pleural effusion are evident.

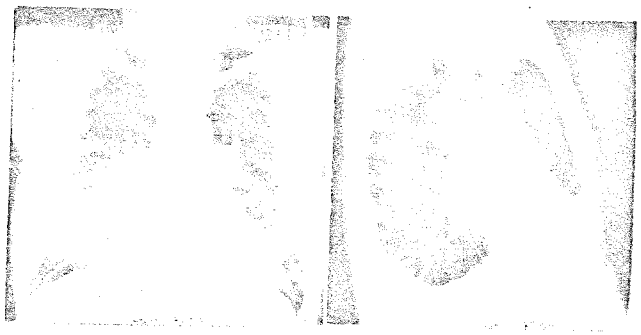

Fig. 6.: Chest x-ray of a patient with congestive cardiomyopathy and severe lung edema.

Sagittal tomograms of both right and left lungs (fig. 7) display a marked increase of lung density, more striking in the paramediastinal planes. The large hilar and lower lobe vessels appear considerably dilated and dense, their shape being obscured by the large amount of edema fluid. Unlike the previous case, the areas of increased lung density extend far beyond the hilar region, thus indicating an extensive recruitment of the extravascular compartment up to the very peripheral tiny interstitial space. On the left side, a thin portion of lung tissue, close to the heart and the diaphragm, is preserved from edema probably as a consequence of the pumping function of these muscular structures.

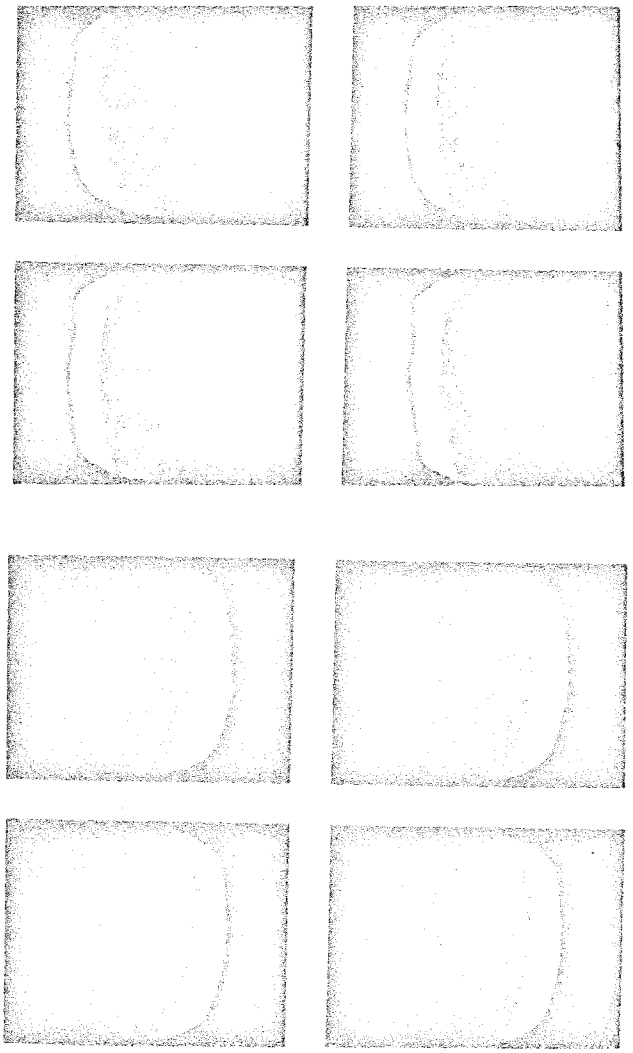

Fig. 7.: Sagittal tomograms of both right (upper panel) and left (lower panel) lungs of the same patient of fig. 6.

As stated before, a computer processing is required in order to clear the original images of

several acquisition errors.
In fig. 8 a digitized image from the right lung of the same patient is shown as it is displayed by the computer before any further processing.

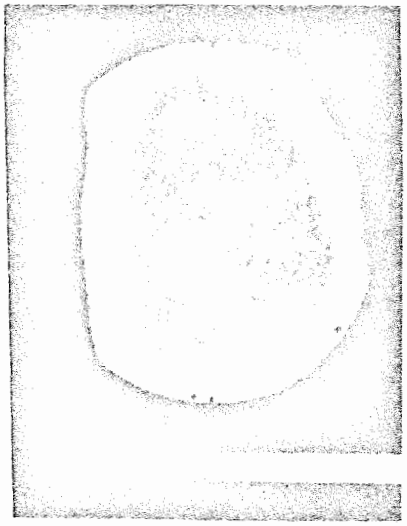

Fig. 8.: Digitized sagittal tomogram without any further processing.

The effect of the primary beam attenuation is clearly seen in the lung regions far away from the radiation source. Moreover there is a considerable degradation of the image contrast, mostly due to the effect of multiple scattering. After the computer analysis is performed (fig. 9), the actual lung tissue density distribution can be visualized throughout the whole depth of the section.

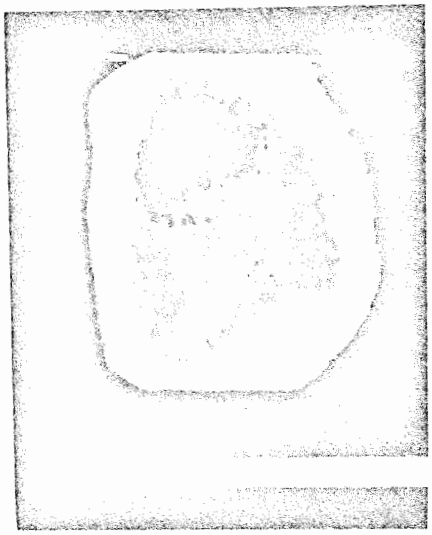

Fig. 9.: The same tomogram after the computer processing.

Gravimetric tissue density values, in a range between 0 and 1 ($g.cm^{-3}$), are displayed by means of either a chromatic or a black and white scale. In order to enhance features of clinical interest, the reference scale can be subdivided into segments, each one covering a known range of density.
The tomographic properties of Compton scattering can be used not only to monitor lung density changes in the course of cardiogenic edema but also to differentiate various types of edema and namely high permeability lung edema from hydrostatic edema. Fig. 10 shows the chest film of a patient who developed an acute respiratory distress syndrome after a traumatic brain injury. Patchy areas of lung consolidation are scattered throughout the right lung.

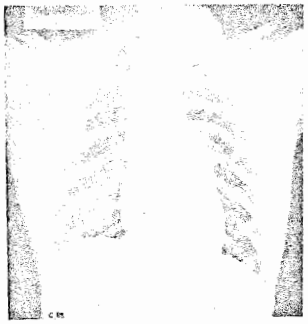

Fig. 10.: Chest x-ray of a patient with acute respiratory distress syndrome.

Chest tomograms reveal focal areas of increased lung density that, unlike cardiogenic edema, are confined to the lung periphery, thus reflecting different patterns of edema fluid accumulation and reabsorption.

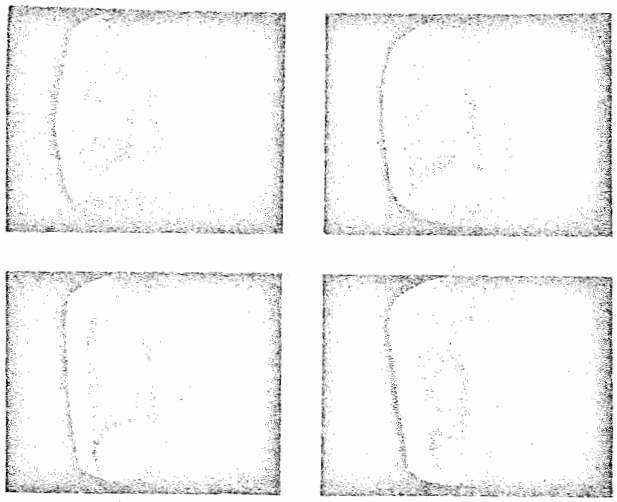

Fig. 11.: Right lung sagittal tomograms of the same patient.

Therefore, these findings, though preliminary, may be used to provide objective criteria for a correct differential diagnosis of these types of lung edema.

References

1. Staub, N.C., Nagano, H., Pearce, M.L. Pulmonary edema in dogs, especially the sequence of fluid accumulation in lungs. J. Appl. Physiol. 22: 227-240, 1967.
2. Pistolesi, M., Giuntini, C.: Assessment of extravascular lung water. Radiol. Clin. North Am. 16: 551-574, 1978.
3. Wegener, O.H., Koeppe, P., Oeser, H.: Measurement of lung density by Computed Tomography. J. Comput. Assist. Tomogr. 2: 263-273, 1978.
4. Gamsu, G., Kauffman, L., Swann, S.J., Brito, C.: Absolute lung density in experimental canine pulmonary edema. Invest. Radiol. 14: 261-268, 1979.
5. Simon, D.S., Murray, J.F., Staub, N.C.: Measurement of pulmonary edema in intact dogs by transthoracic gamma-ray attenuation. J. Appl. Physiol. 47: 1228-1233, 1979.
6. Pistolesi, M., Guzzardi, R., Solfanelli, S., Mey, M., Giuntini, C.: Regional lung density imaging by 90° scattering of an external gamma-ray source. In: Proceedings of the San Diego Biomedical Symposium. Ed. J.I. Martin, Vol. 16, pp. 45-53, New York: Academic Press, 1977.
7. Azzarelli, L., Chimenti, M., Denoth, F., Fabbrini, F.: Chest tomography by Compton scattered radiation: an heuristic enhacement and restoration. In: Proceedings of the International Conference on Image Analysis and Processing. Ed. Cantoni V. pp. 141-147, Pavia: SE.A.G., 1980.
8. Battista, J.J., Santon, L.W., Bronskill, M.J.: Compton scatter imaging of transverse sections: correction for multiple scatter and attenuation. Phys. Med. Biol. 22: 229-244, 1977.